ISSN 1068-1620, Russian Journal of Bioorganic Chemistry, 2020, Vol. 46, No. 6, pp. 1229–1241. © Pleiades Publishing, Ltd., 2020.
Russian Text © The Author(s), 2020, published in Bioorganicheskaya Khimiya, 2020, Vol. 46, No. 6, pp. 770–783.

Increasing the Fluorescence Brightness of Superphotostable EGFP Mutant by Introducing Mutations That Block Chromophore Protonation

A. V. Mamontova[a], A. M. Shakhov[b], A. P. Grigoryev[c], K. A. Lukyanov[d], and A. M. Bogdanov[d, 1]

[a]*Center of Life Sciences, Skolkovo Institute of Science and Technology, Moscow, 121205 Russia*
[b]*Semenov Institute of Chemical Physics, Russian Academy of Sciences, Moscow, 119334 Russia*
[c]*Moscow State University, Moscow, 119234 Russia*
[d]*Shemyakin–Ovchinnikov Institute of Bioorganic Chemistry, Russian Academy of Sciences, Moscow, 117997 Russia*

Received April 21, 2020; revised April 26, 2020; accepted April 30, 2020

Abstract—The design of fluorescent proteins with increased photostability is an important practical task. One of the approaches to its solution is the search for amino acid residues, which play a key role in chromophore-mediated photochemical reactions. The effect of tyrosine-145 on the photooxidation of the chromophore in the EGFP (Enhanced Green Fluorescent Protein) has been previously demonstrated. We have designed the EGFP-Y145L mutant, which has exhibited a significantly reduced efficiency of photooxidation and associated photobleaching. In this work, we are looking for ways to increase the fluorescence brightness of this mutant. For this purpose, we have introduced the S205V and E222G substitutions and their combination to shift the pH equilibrium of the chromophore environment towards ionization of the chromophore. We have shown that both mutants that contain the S205V substitution carry mostly the neutral chromophore, have low brightness, and are capable of slow photoactivation. They may be of interest for studying light-dependent proton transfer. Probably, these proteins can function as time-resolved pH sensors. As we have expected, the chromophore resides in the EGFP-Y145L/E222G mutant is predominantly in the anionic form. The fluorescence brightness of this protein is four times higher than that of the original EGFP-Y145L, and its photostability is higher than that of EGFP by factors of 1.5–5.

Keywords: fluorescent proteins, GFP, photostability, fluorescence spectroscopy, photoinduced oxidation, chromophore, excited state lifetime, ESPT

DOI: 10.1134/S1068162020060187

INTRODUCTION

Proteins of the GFP family, the only class of fluorescent probes encoded by a single gene, occupy a special place among markers in biomedical science. The compatibility of these tags with most expression systems, their stability, relatively low toxicity, and the autocatalytic formation of the chromophore group provided a rapid development of methods of in vivo labeling of biological objects by fluorescent proteins (GFP-revolution [1]). The Nobel Prize in chemistry was awarded for the discovery of GFP and its implementation in scientific practice [2].

Modification of the DNA coding sequence is the main method for obtaining new variants of fluorescent proteins (FPs). In the first years after the cloning of the *avGFP* gene from the *Aequorea victoria* jellyfish and successful demonstration of its expression in heterologous biological systems [3], researchers obtained mutants with improved brightness [4–6] and shifts in fluorescence emission to the blue [7] and red [8] regions of the spectrum. The replacement of only one amino acid (T203H) made it possible to create the first photoactivatable version of GFP [9]. Later, after cloning the genes of red fluorescent proteins from marine corals [10], mutagenesis helped solve the problem of spontaneous oligomerization of these molecules [11, 12]. The rich palette of available fluorescent proteins [13] is mostly filled with artificially developed variants [14, 15].

The design of FPs, especially at the early stages of the GFP revolution, was aimed at improving their basic practical characteristics, i.e., an increase of the fluorescence brightness, the rate of chromophore

Abbreviations: GFP, green fluorescent protein; avGFP, Aequorea victoria green fluorescent protein from *Aequorea victoria*; FP, fluorescent protein; ESPT, excited state proton transfer; EC, extinction coefficient; EGFP, enhanced green fluorescent protein; YFP, yellow fluorescent protein, FLIM, fluorescence lifetime imaging microscopy, QY, quantum yield; PBS, phosphate buffered saline; SMLM, single molecule localization microscopy; PAGFP, photoactivatable GFP.

[1] Corresponding author: phone: +7 (903) 746-08-49; e-mail: noobissat@yandex.ru.

maturation, and the broadening of the spectral diversity of these fluorophores, which are important for the development of multicolor labeling methods [16, 17]. The successful solution of these problems was provided, in particular, by relatively simple algorithms for screening and selection of mutants with the desired properties in the bacterial expression system [7, 12]. The abovementioned mutant of avGFP with increased brightness, EGFP (enhanced green fluorescent protein), was described a year after demonstration of the *avGFP* expression in *E. coli* and *C. elegans*. EGFP was obtained by the two amino acid substitutions in the parental protein. It is noteworthy that EGFP remains one of the most popular green FPs to this day despite the gradual appearance of variants with optimized folding, faster maturation, and significantly increased brightness [18–20]. Thus, the characteristics of EGFP as a label for traditional fluorescence microscopy proved to be adequate for the researchers' requests. Complex experimental models and modern methods of fluorescence imaging made to pay attention to the FP properties previously considered as secondary, i.e., phototoxicity, photoswitching ability, photostability, and the fluorescence lifetime. It turned out that the design of new FP versions with the tuning of these characteristics is a laborious task, if only because it is difficult and sometimes impossible to perform high-content screening and selection of mutants.

One of the specific requirements for fluorophores in superresolution-resolution microscopy (the methods of the SMLM family [21, 22]) and time-resolved microscopy (FLIM [23]) is photostability, i.e., the ability of a molecule to support multiple cycles of light absorption/emission [24]. This ability mainly affects the duration of the experiment (as a function of the specific load of exciting radiation on the sample) in conventional fluorescence microscopy. However, in SMLM and FLIM techniques, individual photons, emitted by the probe, are detected. Therefore, these methods require the enhanced photostability of fluorophores for the goodness of experimental data related to the number of photons [25, 26]. Photostability is highly connected with the bleaching of the FP chromophore due to photochemical processes. The study of photobleaching molecular mechanisms is a basis for the development of new approaches to increase photostability. The literature describes the designing of photostable FPs using directed protein evolution [7, 27, 28] and their rational design based on the study of photobleaching. For example, red FPs, i.e., mKate2 S143C (so-called mStable) and mPlum S146C, have the photostability, which is an order of magnitude higher than that of the parental proteins. This property is due to the stabilization of the chromophore in cis-conformation by the sulfoxide groups, which are formed under photooxidation of the cysteine residue introduced in the protein [29]. Photooxidation of the sulfur-containing residue in photoswitched proteins of the EosFP family was suggested, on the contrary, as a potential channel for the exhaustion of switching capabilities (so-called photofatigue). In fact, the Met159Ala replacement led to a significant increase in the photostability of IrisFP (EosFP homolog) [30]. Finally, when searching for amino acid residues of EGFP, which mediate photooxidation of its chromophore, we identified the key role of Tyr145 as an intermediate electron acceptor. We described the EGFP-Y145L mutant, which demonstrates an approximately ten-fold increase in photostability under microscopy in living cells and an eighty-fold increase after in vitro irradiation of the purified protein under oxidative conditions [31]. At the same time, the Y145L substitution led to a significant shift in the pH balance in the environment of the chromophore group, the domination of the nonfluorescent neutral form of the chromophore (absorption maximum at ~400 nm), and, consequently, a decrease in the brightness of the mutant compared to the original EGFP (Fig. 1). Moreover, EGFP-Y145L is capable of photoactivation (apparently because of light-dependent deprotonation of the chromophore). These factors reduce its value as a photostable marker.

A possible approach to increase the brightness of the EGFP-Y145L is to reduce the efficiency of chromophore protonation, which can presumably be achieved by additional amino acid substitutions described earlier as affecting the acidity of the GFP chromophore.

The serine residue 205 is of interest in the effect on pKa of the GFP chromophore. Owing to interaction with the chromophore-forming Tyr66 residue, mediated by a structural water molecule [32–34], Ser205 plays a significant role in the light-induced excited state proton transfer (ESPT) and affects protonation of the chromophore in the ground state [35]. Mutations in this position can lead to a significant reorganization of the hydrogen bond network in the chromophore environment [36, 37]. For example, the replacement of Ser205 by valine slows down the kinetics of ESPT in avGFP [36–38] and promotes a shift in the pH balance of the chromophore towards deprotonation in SiriusGFP [39]. Moreover, the Ser205Val substitution significantly increased the protein photostability in the case of green SiriusGFP, a close homolog of EGFP, and the mClY chloride sensor based on the yellow fluorescent protein (YFP) that contained the chromophore of the GFP type [36, 40].

The second amino acid residue as a target for mutagenesis in this work is glutamate 222. The substituent at the 222 position is highly conservative in natural FPs and, along with Arg96, is considered an important structural determinant of chromophore maturation [41–43] and stabilization of the mature chromophore in the fluorescent state [32, 43]. Ultimately, this substituent determines the complex of physicochemical characteristics of FPs [44–46]. In terms of our aims, Glu222 is mostly interesting

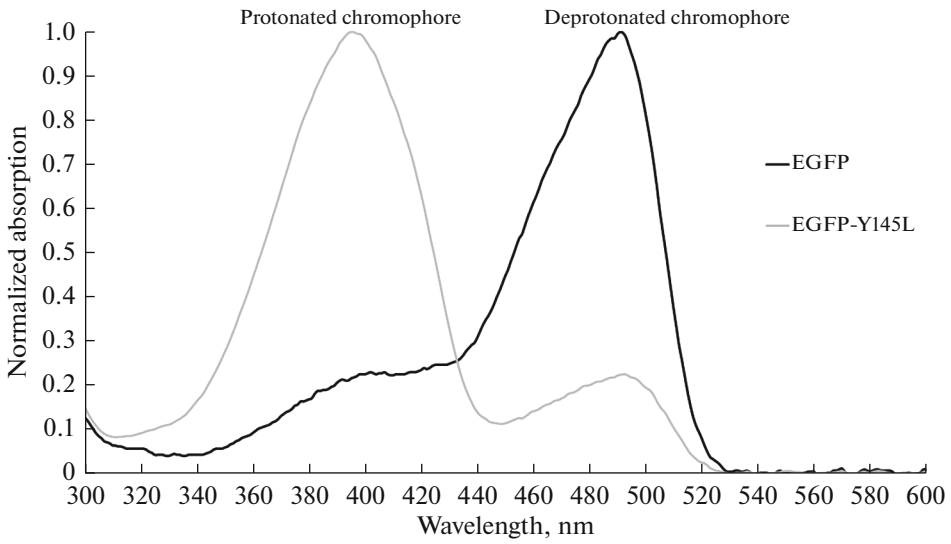

Fig. 1. Absorption spectra of EGFP and EGFP-Y145L proteins.

because of its involvement in the intraprotein proton transfer in both the ground [47] and excited electronic states of the chromophore [33, 34, 42, 48]. In particular, Glu222 is considered to be terminal proton acceptor in the native ESPT chain of avGFP [49]. The replacement of Glu222 by the uncharged glutamine blocks ESPT [49] similar to the S65T mutation of the first amino acid in the chromophore triad (when the latter is introduced, the glutamate carboxyl group is reoriented from the Tyr66 chromophore side [4, 50]). The most interesting for us is the E222G substitution described along with early avGFP mutants, which suppressed the chromophore protonation [32, 52]. Later, the same mutation was revealed in experiments on the directed protein evolution of acGFPL, a colorless GFP-like protein from the *Aequorea coerulescens* hydrozoan jellyfish, which made it possible to obtain bright aceGFP that contained the chromophore in the strictly ionized state at the physiological pH value [53]. E222G can block an additional chromophore photooxidation channel by excluding the potential acceptor (the ionized Glu222 residue) from the electron transfer chain [54]. Our work on the analysis of the amino acid residues involved in light-induced electron transfer in EGFP does not confirm the role of Glu222 [31]. However, if the hypothesis of Saha et al. is true, the E222G mutation can not only contribute to the deprotonation of the chromophore but also improve the photostability of the protein.

RESULTS AND DISCUSSION

Mutation S205V

We assumed that the S205V mutation in EGFP-Y145L can not only shift the pK_a of the chromophore to the acidic region, thus restoring the brightness of the fluorescence due to the predominance of the anionic form, but also preserve a high photostability of the double mutant. The analysis of the spectral properties of EGFP-Y145L/S205V, however, showed that our assumption was incorrect. The absorption spectrum of the spectrum of the double mutant (Fig. 2a) showed the predominant neutral form of the chromophore with the absorption maximum at 395 nm and amplitude, which was 15 times greater than that of the anionic chromophore. The absorption maximum of the latter is shifted by ~10 nm to the red region compared to the corresponding EGFP peak (Fig. 2a, Table 3). The fluorescence spectra (Fig. 2b) show a noticeable (~5 nm) bathochromic shift of the emission maximum (when excited at 470 nm) and a significant (more than 10 nm) shift of the excitation maximum relative to EGFP. EGFP-Y145L/S205V has also a well-pronounced second short-wave excitation maximum (390 nm), which indicates the ESPT process in this mutant and possibly, its ability to photoactivation. When the EGFP-Y145L/S205V fluorescence is excited at 395 nm, both a blue (454 nm) and a green (511 nm) bands are detected in the emission spectrum (Fig. 2c). The difference in the positions of the emission maxima of green fluorescence at the short-wave and long-wave excitation (511 nm vs 516 nm) is a characteristic spectral sign of light-induced proton transfer.

The measurement of the fluorescence lifetime of the EGFP-Y145L and EGFP-Y145L/S205V proteins showed the presence of two major fluorescent fractions in the latter protein with lifetimes of 630–700 ps (depending on the excitation mode) and ~2 ns (Table 1). It is noteworthy that the decay kinetics of the EGFP-Y145L fluorescence both in single-photon and two-photon modes is well approximated by a single-component exponential model with a lifetime of ~2.6 ns close to that of EGFP and corresponds to direct fluo-

Table 1. Kinetic characteristics of fluorescence decay for the EGFP, Y145L, and Y145L/S205V proteins upon excitation of anionic chromophore

Protein	Excitation mode*	τ_1, ps	A_1, %	τ_2, ps	A_2, %
EGFP	1P	2760 ± 6	100	–	–
	2P	2725 ± 7	100	–	–
Y145L	1P	2630 ± 7	100	–	–
	2P	2565 ± 5	100	–	–
Y145L/S205V	1P	1925 ± 20	58	627 ± 10	42
	2P	2070 ± 25	55	710 ± 30	45

*1P, one-photon excitation (490 nm); 2P, two-photon excitation (980 nm).

rescence of the anionic form of the chromophore. Probably, in the case of a double mutant, the fluorescence decay kinetics with a lifetime of 2 ns also characterizes the direct S1–S0 transition of the anionic chromophore (with some quenching because of ESPT), and the short-lived component characterizes the fluorescence of the neutral chromophore in the blue region (~460 nm).

The EGFP-Y145L/S205V mutant is characterized by an extremely low quantum efficiency when excited in the blue region. The extinction coefficient of the anionic form of the chromophore is only 2400 M^{-1} cm^{-1}, and the fluorescence quantum yield (λ_{ex} = 500 nm) is 0.2 (Table 3). Thus, the effective fluorescence brightness of this protein will be ~1% of that for EGFP when using a standard GFP filter set. Our results on fluorescence microscopy of EGFP-Y145L/S205V both in vitro using the protein immobilized on particles of metal affinity resin and in cellulo using the protein expressed in the HEK293T cells confirm the above calculations (data not shown). We have also revealed that the double mutant can be photoactivated (see *Photostability and Photoactivation*).

Mutation E222G

The spectral characteristics of EGFP-Y145L/E222G indicate the desired shift of chromophore acidity towards deprotonation. The amplitude ratio of the absorption peaks of the neutral (λ = 395 nm) and anionic (λ = 488 nm) forms of the chromophore is 1 : 1.4, whereas this ratio for the original EGFP-Y145L is ~4 : 1 (Fig. 3).

The excitation and emission fluorescence spectra of the double mutant are almost identical to those for EGFP (data not shown), and the fluorescence decay kinetics under excitation at 490 nm is well approximated by a single component model with τ ~ 3.1 ns (Table 2). Moreover, we found no evidence of photoactivation of this protein by blue light (470 ± 20 nm) using fluorescence microscopy of the isolated protein (excitation power of ~1 W/cm^2). The relative brightness of the EGFP-Y145L/E222G fluorescence is ~70% of that for EGFP, which is inferior to the latter mainly because of the low fluorescence quantum yield of the anionic form (Table 3). In general, these data indicate the homogeneity of the fluorescent population of EGFP-Y145L/E222G and, consequently, the possibility of using this protein as a fluorescent label in typical experiments. However, according to the spectrophotometric results, the proportion of the EGFP-Y145L/E222G molecules that contain the neutral chromophore was about 40%, thus meaning that almost half of the protein does not fluoresce. We suppose that the incomplete effect of E222G substitution on the EGFP-Y145L chromophore ionization reflects general complexity of the FP properties determination. The chromophore protonation determinants are numerous [49]. Blocking some pathways of the intraprotein proton transfer often leads to the activation of others. Moreover, recent high-resolution structural data on the E222Q mutant (the mutation effect is similar to E222G) show that the protonation state of the Tyr66 in the chromophore is not directly related to the system of hydrogen bonds around Thr65/Gln222 [55]. Assuming that the residual protonation of the chromophore may be associated with the formation of a new network of hydrogen bonds in the chromophore environment and the activation of an alternative proton transfer chain, we hypothesized that serine 205 may play the role of a proton donor or acceptor in the EGFP-Y145L/E222G molecule. To test this assumption, we constructed the EGFP variant that contained three amino acid substitutions, i.e., EGFP-Y145L/S205V/E222G. The spectral properties of this mutant protein are significantly closer to those of EGFP-Y145L/S205V than of EGFP-Y145L/E222G. The absorption spectrum of EGFP-Y145L/S205V/E222G (Fig. 4a) shows the dominant peak of the neutral chromophore (λ_{max} = 394 nm). Its fluorescence in the green region (λ_{max} = 515 nm) is characterized by the bimodal excitation (maxima at 394 and 496 nm), which indicates the ESPT process (Fig. 4b). However, the efficiency of the proton transfer in the excited state is probably low because only the blue peak (~455 nm) is visible in the emission spectrum of the triple mutant when excited at 395 nm (data not shown). EGFP-Y145L/S205V/E222G shows a

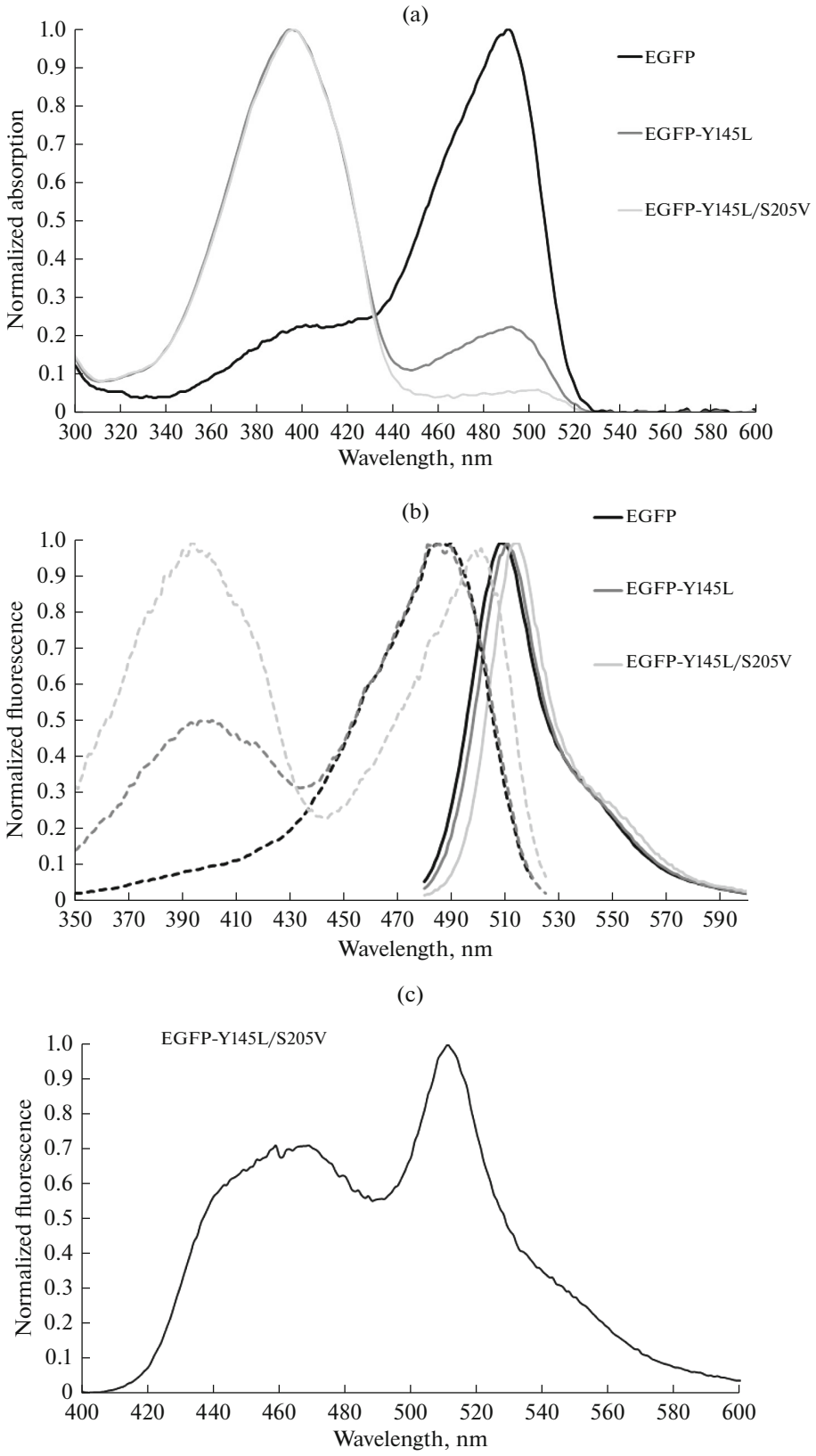

Fig. 2. (a) Absorption spectra of the EGFP, EGFP-Y145L, and EGFP-Y145L/S205V proteins. Absorption maxima of the protonated and deprotonated forms of the chromophore are 395 nm and 490–500 nm, respectively. (b) Fluorescence excitation and emission spectra (dotted line, λ_{ex} = 470 nm and solid line, λ_{em} = 530 nm, respectively) of the same proteins. Ordinate axis: fluorescent signal normalized to the maximal value. (c) The fluorescence emission spectrum of EGFP-Y145L/S205V after excitation at 395 nm. Ordinate axis: fluorescent signal normalized to the maximal value.

Table 2. Kinetic characteristics of fluorescence decay for EGFP-Y145L/E222G, and Y145L/S205V/E222G upon excitation of anionic chromophore

Protein	Excitation mode*	τ_1, ps	A_1, %	τ_2, ps	A_2, %
Y145L/E222G	1P	3190 ± 12	100	–	–
	2P	3080 ± 10	100	–	–
Y145L/S205V/E222G	1P	2310 ± 23	75	644 ± 20	25
	2P	2420 ± 30	64	830 ± 40	36

*1P, one-photon excitation (490 nm); 2P, two-photon excitation (980 nm).

low fluorescence brightness (~2% of EGFP brightness) when excited by blue light (Table 3).

Comparative time-resolved spectroscopy of the EGFP-Y145L/E222G and Y145L/S205V/E222G variants (Table 2) confirms the conclusions made in the analysis of the steady-state spectra. As mentioned above, the double mutant forms the homogenous fraction with monoexponential signal decay ($\tau \sim 3.1$ ns). The triple mutant demonstrates an additional short-lived component, which is probably related to the contribution of blue fluorescence of the neutral chromophore. However, the degree of fluorescence quenching (the lifetime shortening) of the anionic chromophore ($\tau \sim 2.3–2.4$ ns) is less pronounced than that of EGFP-Y145L/S205V, which, along with a relatively small amplitude of the short-wave peak of excitation ($\lambda_{max} = 394$ nm), indicates a reduced efficiency of ESPT of the anionic chromophore compared with that for EGFP-Y145L/S205V.

A high proportion of the protonated chromophore of the EGFP variants that contained the S205V mutation was considered as one of the expected results. For example, a similar spectral pattern was described for the avGFP-S205V protein, which served as a model for studying alternative proton transport pathways in GFP [37]. Moreover, avGFP-S205V/T203V, in which ESPT was completely blocked, does not contain the anionic form of the chromophore at all and fluoresces only in the blue region of the spectrum (459 nm) when the neutral chromophore is excited.

Photostability and Photoactivation

We measured the photobleaching kinetics of all the abovementioned mutant proteins and the parental EGFP under identical experimental conditions (Table 3). The photostability of FPs was evaluated using wide-field fluorescence microscopy and a standard GFP filter set for three model systems (*Microscopy* in *Materials and Methods*). The first of them, the purified protein in a neutral saline buffer, is the standard to evaluate the in vitro photostability [16, 27, 56]. The second system, the protein in the presence of a single-electron acceptor (potassium ferricyanide), has proven itself well for evaluating the contribution to photobleaching of oxidative processes in the excited state [31, 57, 58]. The third system, the protein expressed in the HEK-293T cells, probably most adequately reflects the pho-

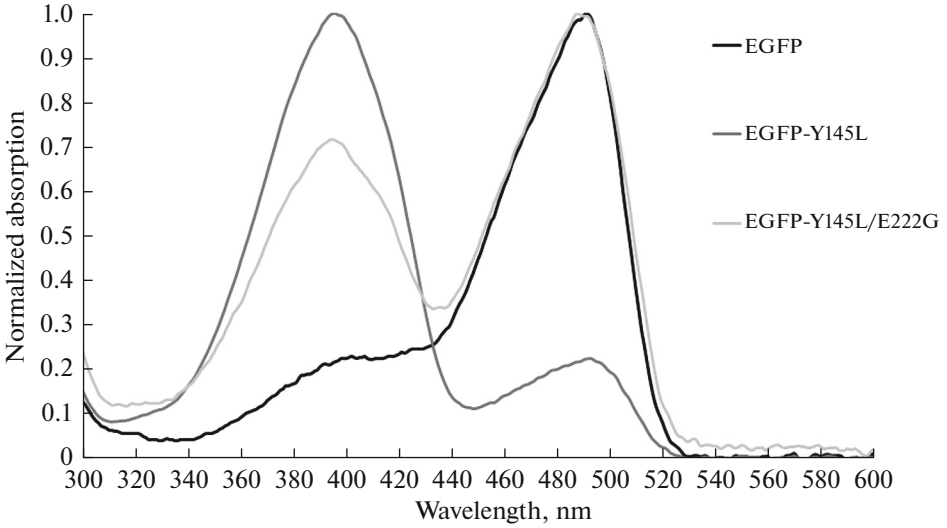

Fig. 3. Absorption spectra of the EGFP, EGFP-Y145L, and EGFP-Y145L/E222G proteins. Absorption maxima of the protonated and deprotonated (anionic) forms of the chromophore are 395 and ~490 nm, respectively.

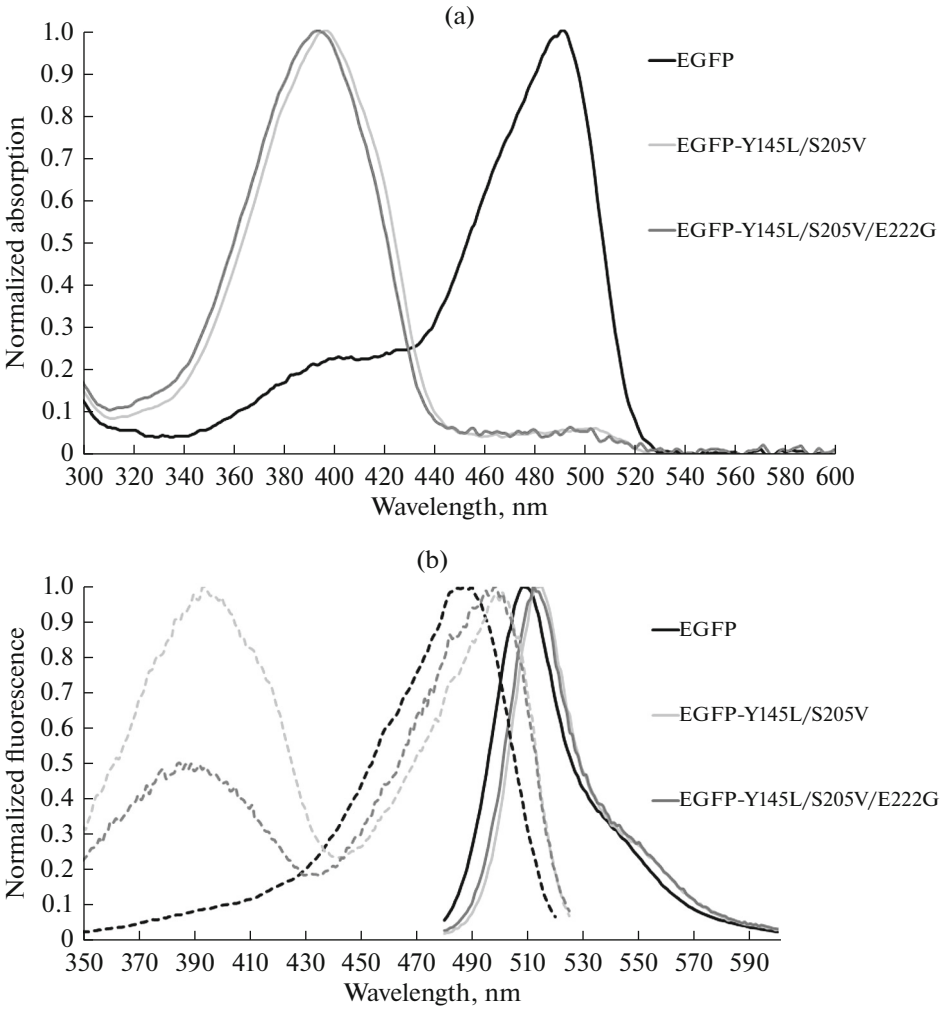

Fig. 4. Absorption spectra of EGFP, EGFP-Y145L/S205V, and EGFP-Y145L/S205V/E222G proteins. (a) Absorption maxima of the protonated and deprotonated forms of the chromophore are 395 nm and 490–500 nm, respectively. (b) Fluorescence excitation and emission spectra (dotted line, λ_{ex} = 470 nm and solid line, λ_{em} = 530 nm, respectively) of the same proteins. Ordinate axis: fluorescent signal normalized to the maximal value.

Table 3. Spectral characteristics and photostability of EGFP and its mutants

Protein	$\lambda_{ex}/\lambda_{em}$, nm	EC, M^{-1} cm^{-1}	QY	RB, %	Photostability[#]		
					in vitro, buffered saline	in vitro, 500 μM potassium ferricyanide	in cellulo, HEK293T cells
EGFP	488/509	55000	0.60	100	2.5 ± 1 min	2.5 ± 0.3 s	35 ± 4 s
EGFP-Y145L	397 and 489/509	10400	0.52	16	7 ± 2 min	45 ± 7 s	3.5 ± 1 min
EGFP-Y145L/E222G	483/509	65000	0.36	71	3.5 ± 1 min	12 ± 1.7 s	1 ± 0.5 min
EGFP-Y145L/S205V	390 and 501/516	2400	0.20	1.5	35 ± 5 min	10 ± 2 min	9 ± 3 min
EGFP-Y145L/S205V/E222G	394 and 496/515	2100	0.30	1.9	31 ± 8 min	23 ± 5 min	5 ± 2 min

EC, the extinction coefficient of anionic form of protein chromophore; QY, the quantum yield of fluorescence; RB, relative protein brightness. Relative brightness is calculated as the product of the molar extinction coefficient and the quantum yield of fluorescence and is given in comparison with the brightness of EGFP. [#]Photostability refers to the time, which is required for decreasing fluorescence intensity by 50%. Photostability in the cells was evaluated at $N \geq 20$.

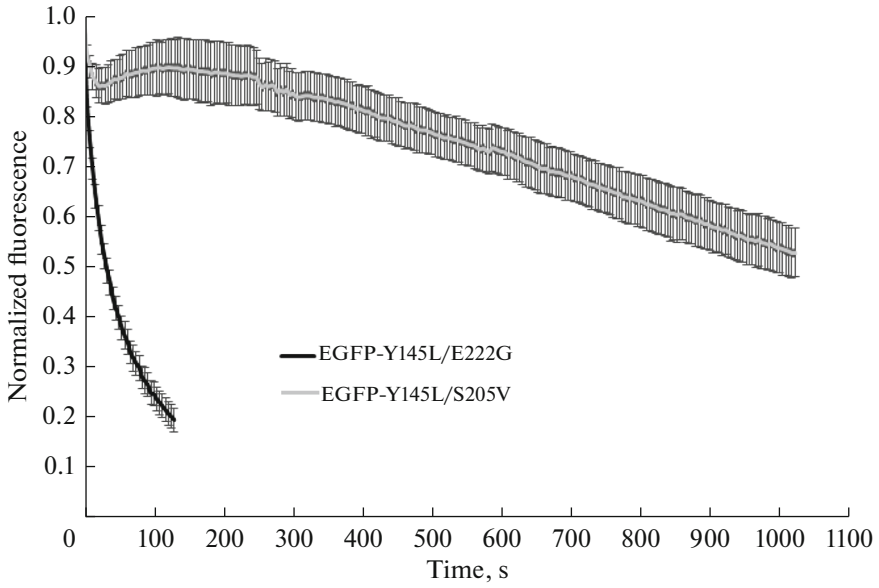

Fig. 5. Kinetics of the change in fluorescence intensity of the EGFP-Y145L/E222G, and EGFP-Y145L/S205V proteins in vitro in the presence of $K_3[Fe(CN)_6]$ (500 μM). $N = 10$.

tostability of the marker under conditions of biological imaging. It should be noted that the comparison of the experimental values is possible only within the data for each model system.

The characteristics of the EGFP-Y145L protein during the photobleaching have been described earlier in detail [31], and the data presented here generally repeat previous results. EGFP-Y145L is extremely resistant to bleaching but its weak photoactivation, when exposed to broadband blue light, leads to some overestimation of the observed photostability. The EGFP-Y145L/E222G imaging required settings of detector sensitivity almost identical to those for EGFP. At a brightness comparable to the parental protein, this mutant demonstrated significantly increased photostability relative to EGFP in all three model systems, i.e., ~1.5 times higher in the salt buffer, ~5 times higher in the presence of the oxidant, and ~2 times higher in the living cells. We would associate this effect (the slowdown of EGFP-Y145L/E222G photobleaching under oxidative conditions in vitro) with the role of the Y145L mutation in blocking light-induced electron transfer. Both mutant variants that contain the S205V substitution are noticeably activated when measuring the photobleaching kinetics (Fig. 5). For this reason, the characteristic values of the photobleaching time for EGFP-Y145L/S205V and EGFP-Y145L/S205V/E222G (Table 3) reflect the apparent rather than true photostability of these fluorophores. These properties of both proteins, along with their low brightness, makes them unsuitable for routine fluorescent imaging.

However, photoactivation of the mutants with the S205V substitution may be of some interest to the scientific community, for example in the context of SMLM methods. It is reasonable to assume that the observed photoactivation is associated with light-induced deprotonation of the chromophore, which is initiated by the protein absorption in the violet region of the spectrum (in fluorescence microscopy, we use a BP470/40 filter for excitation). The deprotonation mechanism may be similar to that of the well-characterized photoactivation of the PAGFP protein (EGFP-T203H) [59–62]. During this process, ESPT-induced chromophore ionization is accompanied by decarboxylation of the Glu222 side chain, followed by a rearrangement of the hydrogen bond network that favors the stabilization of the anionic form of the chromophore. However, decarboxylation of Glu222 in EGFP-Y145L/S205V/E222G is not possible. Besides, an important structural determinant of this stabilization is the stacking interaction of the His203 residue with the chromophore [9], which is absent in our proteins. Probably, an alternative photoactivation scenario is fulfilled in the EGFP-Y145L/S205V and EGFP-Y145L/S205V/E222G mutants, the study of which requires additional structural studies.

To evaluate the effectiveness and determine the spectral features of the photoactivation, we irradiated an aqueous solution of purified EGFP-Y145L/S205V/E222G with intense violet light and recorded the absorption spectrum of the solution at regular intervals (Fig. 6).

The excitation of the neutral form of the chromophore leads to a gradual increase in the population of the anionic chromophore molecules (λ_{abs} = 495 nm). The photoactivation of EGFP-Y145L/S205V/E222G is not a very effective process, i.e., the absorption of

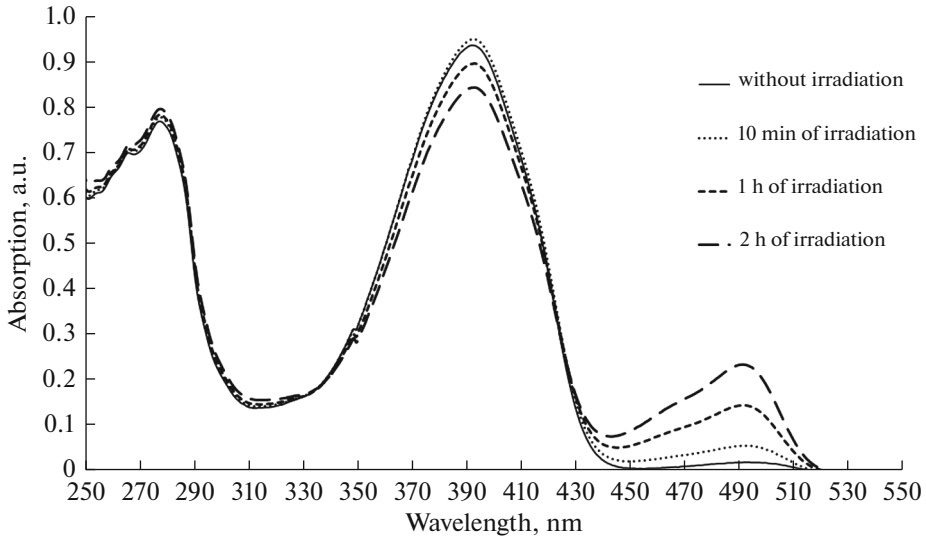

Fig. 6. Absorption spectra of the EGFP-Y145L/S205V/E222G mutant after irradiation of the protein sample with short-wave intense light (405 nm, ~5.5 W/cm^2).

the anionic form of the chromophore increased only by factors of 3–4 for 2 h of irradiation (for comparison, UV photoactivation of the aceGFP-G222E mutant achieved a 1000-fold increase in the fluorescent signal [53]).

CONCLUSIONS

We have examined the introduction of two amino acid substitutions, S205V and E222G, which are the important determinants of acidity of the GFP chromophore. We have also studied the combinations of these two substitutions to increase the brightness of the photostable EGFP-Y145L mutant.

The S205V mutation did not meet our expectations; it shifts the pKa of the chromophore to the alkaline region and promotes the chromophore protonation and the ESPT process. On the other hand, the mutant proteins with this substitution may be interesting for studying the ESPT kinetics (this process in EGFP-Y145L/S205V proceeds, probably, with the use of an alternative proton transfer channel). The EGFP-Y145L/S205V and EGFP-Y145L/S205V/E222G mutants are photoactivatable fluorescent proteins, which presumably use a previously undescribed photoactivation mechanism. The properties of these mutants can be used in SMLM. Finally, the properties of variants that contain the S205V substitution, i.e., complex photobehavior in the time domain, the high contribution of short-lived fluorescent populations to the pool of registered photons, and the pronounced protonation of the chromophore at neutral pH, opens up the prospect of their use as time-resolved pH sensors, especially in the alkaline range. On the contrary, the effect of the E222G mutation in EGFP-Y145L met our requirements. The double EGFP-Y145L/S205V/E222G mutant is a relatively bright FP, which retains a 1.5–5-fold increased photostability compared to the parent EGFP.

EXPERIMENTAL

Site-Directed Mutagenesis

The EGFP mutants were prepared by the overlap-extension PCR method using the following set of oligonucleotides that contained the corresponding substitutions. The terminal primers: forward, 5'-ATGCGGATCCATGGTGAGCAAGGGCGAG-3' and reversed 5'-ATGCAAGCTTTTACTTGTACAGCTCGTC-3' for all EGFP mutants; forward 5'-GAGTACAACCTGAACAGCCAC-3' and reversed 5'-GTGGCTGTTCAGGTTGTACTC-3' for EGFP Y145L; forward 5'-GTCCTGCTGGGCTTCGTGACC-3' and reversed 5'-GGTCACGAAGCCCAGCAGGAC-3' for EGFP-E222G; forward 5'-AGCACCCAGGTCGCCCTGAGC-3' and reversed 5'-GCTCAGGGCGACCTGGGTGCT-3' for EGFP-S205V.

The amplified PCR fragment that contained the BamHI/HindIII restriction sites at the end and the coding FP variant was cloned in the pQE30 vector (Qiagen) for bacterial expression.

Expression and Purification of the Protein

The EGFP and the EGFP mutants that contained the 6His tag at the N termini were cloned in the pQE30 vector (Qiagen), expressed in the *E. coli* XL1 Blue strain (Invitrogen), and purified using metal-affinity TALON resin (Clontech).

Vector EGFP-N1 (Clontech) was used for expression in mammalian cells. The EGFP mutants were cloned in EGFP-N1 instead of EGFP. The HEK293T cells (ATCC) were transfected with the above constructs to obtain transient protein expression.

Spectroscopy and Evaluation of Fluorescence Brightness

The absorption and excitation/emission spectra were recorded on a Cary 100 UV/VIS and fluorescent Cary Eclipse spectrophotometers (Varian), respectively. The fluorescence brightness was evaluated as the product of the molar extinction coefficient and the fluorescence quantum yield. All experiments with the native proteins were performed in phosphate-buffered saline (PBS, pH 7.4, GIBCO). The molar extinction coefficient was evaluated by concentration of the mature chromophore. EGFP and its mutants were denatured with 1 NaOH. The GFP-like chromophore is known to absorb under these conditions at 447 nm with the extinction coefficient of 44000 M^{-1} cm^{-1}. The absorption values of the native and denatured proteins were used to calculate the molar extinction coefficients for the native states. To evaluate the fluorescence quantum yield, the areas under the curve of the mutant fluorescence emission spectra were compared with those for EGFP with the same absorption (quantum yield 0.60).

Microscopy

The wide-field fluorescence microscopy was performed using a Leica AF6000 LX imaging system equipped with a CCD Photometrics CoolSNAP HQ camera. The fluorescent images were obtained using an oil immersion lens 63× NA1.4 and a standard set of GFP filters (excitation BP470/40, emission BP 525/50). The fluorescent proteins immobilized on the TALON resin, live embryonic human kidney cells 293 (HEK293T) cultured in DMEM (also visualized in DMEM), and target proteins expressing in the cytoplasm were visualized and bleached using the following settings: 25–50 mW/cm^2 and exposure for 10–100 ms for signal detection and ~1 W/cm^2 and exposure for 5 s for photobleaching. Photobleaching was observed during time-lapse imaging, i.e., by alternating imaging at the low light intensity with exposure to radiation of maximum intensity (using a set of GFP filters). Images were obtained and quantified using the Leica LAS AF software.

Fluorescence Lifetime Imaging Microscopy of Purified Proteins Under Single-Photon and Two-Photon Excitation

The fluorescent proteins that contain anionic chromophores are characterized by discrepancies in spectral properties for one-photon and two-photon absorption [63]. Differences in the kinetic characteristics of fluorescence decay have also been described, which depend on the excitation mode of green FPs of several spectral forms and light-dependent transitions between these forms [64]. Therefore, to expand the scope of the analysis of the time-resolved signal, we measured the fluorescence decay of all proteins in both one-photon and two-photon modes. Femtosecond laser pulses (frequency, 80 MHz; 100 fs; up to 25 nJ/pulse) from a Titanium-Sapphire oscillator (Tsunami, Spectra-Physics) pumped by a continuous green Nd:YVO_4 laser (532 nm, Millennia Prime 6sJ, Spectra-Physics) were converted to the second harmonic in a nonlinear barium borate crystal (BBO, Model 3980, Spectra-Physics). Femtosecond laser pulses at the fundamental wavelength were combined with second-harmonic radiation through a long-wave dichroic mirror (DMLP650, Thorlabs). Combined laser beams were fed into an Olympus IX71 inverted optical microscope through a dielectric filter (FESH0750, Thorlabs) set at an angle of 45° and focused with a lens (40× NA0.75 UPlanFLN, Olympus) on a sample that was placed on a three-coordinate table. Only one of the laser beams was open in each experiment. The samples were prepared as drops of purified fluorescent proteins in PBS, pH 7.4 (GIBCO) applied to a standard 24 × 24 mm cover glass (Heinz Herenz, Germany). The average laser power reaching the sample was precisely tuned using a polarizing attenuator, which consisted of a half-wave plate and a polarizing cube in each of the beams. One-photon fluorescence excitation in the sample was performed by second-harmonic radiation at an average power of up to 10 μW at 490 nm. Two-photon excitation was performed at 980 nm and an average laser power of up to 10 mW. The fluorescence of the sample excited by a femtosecond laser in both modes passed back through the lens and the filter that started the laser radiation. It was then directed to the input of an Acton SP300i polychromator with two separate outputs. A PI-MAX 2 (Princeton Instruments) CCD camera at the first output of the monochromator was used to register the fluorescence spectra. The photoelectric multiplier of the SPC-730 time-correlated photon counting system (Becker & Hickl GmbH) at the second output detected the kinetics of the fluorescence decay in the spectral range of 510–530 nm. The fluorescence lifetime data were obtained using the SPC Image NG software (Becker & Hickl, Germany), exported in the ASCII format, and analyzed using the Origin Pro 9 software (OriginLab, United States).

ACKNOWLEDGMENTS

Experiments were partially performed using the equipment of the Core Facility (CKP) at the Institute of Bioorganic Chemistry, RAS (supported by the grant RFMEFI-62117X0018 of Ministry of Education and Science of Rus-

sia) and the Core Facility (CKP) at the Institute of Chemical Physics, RAS (CKP 506694).

FUNDING

The work was supported by the Russian Foundation of Basic Research (grant no. 19-04-00845 for genetic engineering and fluorescence microscopy and grant no. 19-34-60019 for steady-state and time-resolved spectroscopy).

COMPLIANCE WITH ETHICAL STANDARDS

This article does not contain any studies with the use of humans as objects of research.

Conflict of Interests

The authors state that there is no conflict of interest.

REFERENCES

1. van Roessel, P. and Brand, A.H., *Nat. Cell. Biol.*, 2002, vol. 4, pp. 15–20. https://doi.org/10.1038/ncb0102-e15
2. Shimomura, O., *Angew. Chem., Int. Ed. Engl.*, 2009, vol. 48, pp. 5590–5602. https://doi.org/10.1002/anie.200902240
3. Chalfie, M., Tu, Y., Euskirchen, G., Ward, W.W., and Prasher, D.C., *Science*, 1994, vol. 263, pp. 802–805. https://doi.org/10.1126/science.8303295
4. Heim, R., Cubitt, A.B., and Tsien, R.Y., *Nature*, 1995, vol. 373, pp. 663–664. https://doi.org/10.1038/373663b0
5. Zhang, G., Gurtu, V., and Kain, S.R., *Biochem. Biophys. Res. Commun.*, 1996, vol. 227, pp. 707–711. https://doi.org/10.1006/bbrc.1996.1573
6. Tsien, R.Y., *Annu. Rev. Biochem.*, 1998, vol. 67, pp. 509–544. https://doi.org/10.1146/annurev.biochem.67.1.509
7. Ai, H.W., Shaner, N.C., Cheng, Z., Tsien, R.Y., and Campbell, R.E., *Biochemistry*, 2007, vol. 46, pp. 5904–5910. https://doi.org/10.1021/bi700199g
8. Kremers, G.J., Goedhart, J., van Munster, E.B., and Gadella, T.W., *Biochemistry*, 2006, vol. 45, pp. 6570–6580. https://doi.org/10.1021/bi0516273
9. Henderson, J.N., Gepshtein, R., Heenan, J.R., Kallio, K., Huppert, D., and Remington, S.J., *J. Am. Chem. Soc.*, 2009, vol. 131, pp. 4176–4177. https://doi.org/10.1021/ja808851n
10. Matz, M.V., Fradkov, A.F., Labas, Y.A., Savitsky, A.P., Zaraisky, A.G., Markelov, M., and Lukyanov, S.A., *Nat. Biotechnol.*, 1999, vol. 17, pp. 969–973. https://doi.org/10.1038/13657
11. Shcherbo, D., Murphy, C.S., Ermakova, G.V., Solovieva, E.A., Chepurnykh, T.V., Shcheglov, A.S., Verkhusha, V.V., Pletnev, V.Z., Hazelwood, K.L., Roche, P.M., Lukyanov, S., Zaraisky, A.G., Davidson, M.W., and Chudakov, D.M., *Biochem. J.*, 2009, vol. 418, pp. 567–574. https://doi.org/10.1042/BJ20081949
12. Bindels, D.S., Haarbosch, L., van Weeren, L., Postma, M., Wiese, K.E., Mastop, M., Aumonier, S., Gotthard, G., Royant, A., Hink, M.A., and Gadella, T.W., *Nat. Methods*, 2016, vol. 14, pp. 53–56. https://doi.org/10.1038/nmeth.4074
13. www.fpbase.org/.
14. Nguyen, A.W. and Daugherty, P.S., *Nat. Biotechnol.*, 2005, vol. 23, pp. 355–360. https://doi.org/10.1038/nbt1066
15. Goedhart, J., von Stetten, D., Noirclerc-Savoye, M., Lelimousin, M., Joosen, L., Hink, M.A., van Weeren, L., Gadella, T.W., Jr., and Royant, A., *Nat. Commun.*, 2012, vol. 3, p. 751. https://doi.org/10.1038/ncomms1738
16. Shaner, N.C., Steinbach, P.A., and Tsien, R.Y., *Nat. Methods*, 2005, vol. 2, pp. 905–909. https://doi.org/10.1038/nmeth819
17. Chudakov, D.M., Matz, M.V., Lukyanov, S., and Lukyanov, K.A., *Physiol. Rev.*, 2010, vol. 90, pp. 1103–1163. https://doi.org/10.1152/physrev.00038.2009
18. Pedelacq, J.-D., Cabantous, S., Tran, T., Terwilliger, T.C., and Waldo, G.S., *Nat. Biotechnol.*, 2005, vol. 24, pp. 79–88. https://doi.org/10.1038/nbt1172
19. Cubitt, A.B., Woollenweber, L.A., and Heim, R., *Methods Cell Biol.*, 1998, vol. 58, pp. 19–30. https://doi.org/10.1016/s0091-679x(08)61946-9
20. Shaner, N.C., Lambert, G.G., Chammas, A., Ni, Y., Cranfill, P.J., Baird, M.A., Sell, B.R., Allen, J.R., Day, R.N., Israelsson, M., Davidson, M.W., and Wang, J., *Nat. Methods*, 2013, vol. 10, pp. 407–409. https://doi.org/10.1038/nmeth.2413
21. Jradi, F.M. and Lavis, L.D., *ACS Chem. Biol.*, 2019, vol. 14, pp. 1077–1090. https://doi.org/10.1021/acschembio.9b00197
22. Yan, R., Moon, S., Kenny, S.J., and Xu, K., *Acc. Chem. Res.*, 2018, vol. 51, pp. 697–705. https://doi.org/10.1021/acs.accounts.7b00545
23. De Los Santos, C., Chang, C.W., Mycek, M.A., and Cardullo, R.A., *Mol. Reprod. Dev.*, 2015, vol. 82, pp. 587–604. https://doi.org/10.1002/mrd.22501
24. Mamontova, A.V., Grigoryev, A.P., Tsarkova, A.S., Lukyanov, K.A., and Bogdanov, A.M., *Russ. J. Bioorg. Chem.*, 2017, vol. 43, pp. 625–633. https://doi.org/10.7868/S0132342317060021
25. Seefeldt, B., Kasper, R., Seidel, T., Tinnefeld, P., Dietz, K.J., Heilemann, M., and Sauer, M., *J. Biophotonics*, 2008, vol. 1, pp. 74–82. https://doi.org/10.1002/jbio.200710024
26. Duan, C., Adam, V., Byrdin, M., Ridard, J., Kieffer-Jaquinod, S., Morlot, C., Arcizet, D., Demachy, I., and Bourgeois, D., *J. Am. Chem. Soc.*, 2013, vol. 135, pp. 15841–15850. https://doi.org/10.1021/ja406860e

27. Shaner, N.C., Lin, M.Z., McKeown, M.R., Steinbach, P.A., Hazelwood, K.L., Davidson, M.W., and Tsien, R.Y., *Nat. Methods*, 2008, vol. 5, pp. 545–551. https://doi.org/10.1038/nmeth.1209

28. Zhong, S., Navaratnam, D., and Santos-Sacchi, J., *PLoS One*, 2014, vol. 9, e99095. https://doi.org/10.1371/journal.pone.0099095

29. Ren, H., Yang, B., Ma, C., Hu, Y.S., Wang, P.G., and Wang, L., *ACS Chem. Biol.*, 2016, vol. 11, pp. 2679–2684. https://doi.org/10.1021/acschembio.6b00579

30. Duan, C., Byrdin, M., El Khatib, M., Henry, X., Adam, V., and Bourgeois, D., *Methods Appl. Fluoresc.*, 2015, vol. 3, p. 014004. https://doi.org/10.1088/2050-6120/3/1/014004

31. Bogdanov, A.M., Acharya, A., Titelmayer, A.V., Mamontova, A.V., Bravaya, K.B., Kolomeisky, A.B., Lukyanov, K.A., and Krylov, A.I., *J. Am. Chem. Soc.*, 2016, vol. 138, pp. 4807–4817. https://doi.org/10.1021/jacs.6b00092

32. Ormo, M., Cubitt, A.B., Kallio, K., Gross, L.A., Tsien, R.Y., and Remington, S.J., *Science*, 1996, vol. 273, pp. 1392–1395. https://doi.org/10.1126/science.273.5280.1392

33. Brejc, K., Sixma, T.K., Kitts, P.A., Kain, S.R., Tsien, R.Y., Ormo, M., and Remington, S.J., *Proc. Natl. Acad. Sci. U. S. A.*, 1997, vol. 94, pp. 2306–2311. https://doi.org/10.1073/pnas.94.6.2306

34. Palm, G.J., Zdanov, A., Gaitanaris, G.A., Stauber, R., Pavlakis, G.N., and Wlodawer, A., *Nat. Struct. Biol.*, 1997, vol. 4, pp. 361–365. https://doi.org/10.1016/s0076-6879(00)05489-6

35. Kennis, J.T.M., Larsen, D.S., van Stokkum, I.H.M., Vengris, M., van Thor, J.J., and van Grondelle, R., *PNA*, vol. 101, pp. 17988–17993. https://doi.org/10.1073/pnas.0404262102

36. Zhong, S., Navaratnam, D., and Santos-Sacchi, J., *PLoS One*, 2014, vol. 9, e99095. https://doi.org/10.1371/journal.pone.0099095

37. Shu, X., Leiderman, P., Gepshtein, R., Smith, N.R., Kallio, K., Huppert, D., and Remington, S.J., *Protein Sci.*, 2007, vol. 16, pp. 2703–2710. https://doi.org/10.1110/ps.073112007

38. Simkovitch, R., Huppert, A., Huppert, D., Remington, S.J., and Miller, Y., *J. Phys. Chem. B*, 2013, vol. 117, pp. 11921–11931. https://doi.org/10.1021/jp405698g

39. Laptenok, S.P., Lukacs, A., Gil, A., Brust, R., Sazanovich, I.V., Greetham, G.M., Tonge, P.J., and Meech, S.R., *Angew. Chem., Int. Ed. Engl.*, 2015, vol. 54, pp. 9303–9307.

40. Zhong, S., Rivera-Molina, F., Rivetta, A., Toomre, D., Santos-Sacchi, J., and Navaratnam, D., *J. Neurosci. Methods*, 2019, vol. 313, pp. 68–76. https://doi.org/10.1002/anie.201503672

41. Barondeau, D.P., Putnam, C.D., Kassmann, C.J., Tainer, J.A., and Getzoff, E.D., *Proc. Natl. Acad. Sci. U. S. A.*, 2003, vol. 100, pp. 12111–12116. https://doi.org/10.1073/pnas.2133463100

42. Sniegowski, J.A., Lappe, J.W., Patel, H.N., Huffman, H.A., and Wachter, R.M., *J. Biol. Chem.*, 2005, vol. 280, pp. 26248–26255.

43. Craggs, T.D., *Chem. Soc. Rev.*, 2009, vol. 38, pp. 2865–2875. https://doi.org/10.1039/b903641p

44. Lin, C.Y., Romei, M.G., Oltrogge, L.M., Mathews, I.I., and Boxer, S.G., *J. Am. Chem. Soc.*, 2019, vol. 141, pp. 15250–15265. https://doi.org/10.1021/jacs.9b07152

45. Nakano, H., Okumura, R., Goto, C., and Yamane, T., *Biotech. Bioproc. Eng.*, 2002, vol. 7, pp. 311–315. https://doi.org/10.1007/BF02932841

46. Banerjee, S., Schenkelberg, C.D., Jordan, T.B., Reimertz, J.M., Crone, E.E., Crone, D.E., and Bystroff, C., *Biochemistry*, 2017, vol. 56, pp. 736–747. https://doi.org/10.1021/acs.biochem.6b00800

47. Brejc, K., Sixma, T.K., Kitts, P.A., Kain, S.R., Tsien, R.Y., Ormo, M., and Remington, S.J., *Proc. Natl. Acad. Sci. U. S. A.*, 1997, vol. 94, pp. 2306–2311. https://doi.org/10.1073/pnas.94.6.2306

48. Oltrogge, L.M., Wang, Q., and Boxer, S.G., *Biochemistry*, 2014, vol. 53, p. 5947. https://doi.org/10.1021/bi500147n

49. Agmon, N., *Biophys. J.*, 2005, vol. 88, pp. 2452–2461. https://doi.org/10.1529/biophysj.104.055541

50. Stoner-Ma, D., Jaye, A.A., Matousek, P., Towrie, M., Meech, S.R., and Tonge, P.J., *J. Am. Chem. Soc.*, 2005, vol. 127, pp. 2864–2865. https://doi.org/10.1021/ja042466d

51. Arpino, J.A., Rizkallah, P.J., and Jones, D.D., *PLoS One*, 2012, vol. 7, e47132. https://doi.org/10.1371/journal.pone.0047132

52. Ehrig, T.F.G.P. and O'Kane, D.J., *FEBS Lett.*, 1995, vol. 367, pp. 163–166. https://doi.org/10.1016/0014-5793(95)00557-p

53. Gurskaya, N.G., Fradkov, A.F., Pounkova, N.I., Staroverov, D.B., Bulina, M.E., Yanushevich, Y.G., Labas, Y.A., Lukyanov, S., and Lukyanov, K.A., *Biochem. J.*, 2003, vol. 373, pp. 403–408. https://doi.org/10.1042/BJ20021966

54. Saha, R., Verma, P.K., Rakshit, S., Saha, S., Mayor, S., and Pal, S.K., Sci. *Rep.*, 2013, vol. 3, pp. 1–7. https://doi.org/10.1038/srep01580

55. Takaba, K., Tai, Y., Eki, H., Dao, H.A., Hanazono, Y., Hasegawa, K., Miki, K., and Takeda, K., *IUCr J.*, 2019, vol. 6, pp. 387–400. https://doi.org/10.1107/S205225251900246X

56. Shaner, N.C., Campbell, R.E., Steinbach, P.A., Giepmans, B.N., Palmer, A.E., and Tsien, R.Y., *Nat. Biotechnol.*, 2004, vol. 22, pp. 1567–1572. https://doi.org/10.1038/nbt1037

57. Bogdanov, A.M., Mishin, A.S., Yampolsky, I.V., Belousov, V.V., Chudakov, D.M., Subach, F.V., Verkhusha, V.V., Lukyanov, S., and Lukyanov, K.A., *Nat. Chem. Biol.*, 2009, vol. 5, pp. 459–461. https://doi.org/10.1038/nchembio.174

58. Sen, T., Mamontova, A.V., Titelmayer, A.V., Shakhov, A.M., Astafiev, A.A., Acharya, A., Lukyanov, K.A., Krylov, A.I., and Bogdanov, A.M., *Int. J. Mol. Sci.*, 2019, vol. 20, p. 5229. https://doi.org/10.3390/ijms20205229

59. Patterson, G.H. and Lippincott-Schwartz, J., *Science*, 2002, vol. 297, pp. 1873–1877. https://doi.org/10.1126/science.1074952

60. van Thor, J.J., Gensch, T., Hellingwerf, K.J., and Johnson, L.N., *Nat. Struct. Biol.*, 2002, vol. 9, p. 37. https://doi.org/10.1038/nsb739

61. Bell, A.F., Stoner-Ma, D., Wachter, R.M., and Tonge, P.J., *J. Am. Chem. Soc.*, 2003, vol. 125, pp. 6919–6926. https://doi.org/10.1021/ja034588w

62. Shcherbakova, D.M. and Verkhusha, V.V., *Curr. Opin. Chem. Biol.*, 2014, vol. 20, pp. 60–68. https://doi.org/10.1016/j.cbpa.2014.04.010

63. Drobizhev, M., Makarov, N.S., Tillo, S.E., Hughes, T.E., and Rebane, A., *Nat. Methods*, 2011, vol. 8, pp. 393–399. https://doi.org/10.1038/nmeth.1596

64. Volkmer, A., Subramaniam, V., Birch, D.J., and Jovin, T.M., *Biophys. J.*, 2000, vol. 78, pp. 1589–1598. https://doi.org/10.1016/S0006-3495(00)76711-7

Translated by A. Levina